Advances in Nano Research, *Vol. 18, No. 5 (2025) 433-443*
https://doi.org/10.12989/anr.2025.18.5.433

The effect of ethanol-polyvinylpyrrolidone dielectric on the characteristics of silver nano-powders synthesized by electro-discharge process

Xinyu Bai**[1], Hanyu Rao[1], Nidhal Becheikh[2] and Farhad Kiarasi*[3]

[1]*College of Materials Science and Engineering, Nanjing Tech University, Nanjing, 211816, China*
[2]*Department of Chemical and Materials Engineering, Engineering College, Northern Border University, Arar, Saudi Arabia*
[3]*Department of Mechanical Engineering, University of Eyvanekey, Eyvanekey, Semnan, Iran*

(*Received April 10, 2023, Revised October 13, 2024, Accepted October 14, 2025*)

Abstract. In this study, silver nano-particles (AgNPs) were synthesized by an electro-discharge process between two immersed silver electrodes in four dielectrics: 1) Ethanol, 2) Ethanol-3% PVP, 3) Ethanol-5% PVP, and 4) Ethanol-8% PVP. Further, the effect of input parameters of the process was investigated (current intensity, pulse time duration, and PVP concentration) on the powder rate, structure, phases, morphological characteristics, size distribution, and shape of nanoparticles and then compared by XRD, TEM, UV-Vis, PSA, and SEM tests. The results indicated that the synthesized powder rate rose by increasing the current intensity, pulse time duration, and PVP concentration. By increasing the PVP concentration in ethanol, the pulse time duration and current intensity, the size of the silver nanoparticles shrank. Also, with elevation of PVP concentration in ethanol, the stabilization and dispersion of silver nanoparticles increased and improved, while agglomeration diminished. XRD patterns indicated that the synthesis of silver nanoparticles by electro-discharge process prevents formation of undesirable oxide silver phase. Eventually, the optimum values of input parameters for the synthesis of silver nanoparticles with smallest diameter (25nm-50 nm), best dispersion, stabilization, and the minimum agglomeration were obtained as: Ti = 100 (μs), I = 64(A), and PVP with 50 mL concentration in ethanol.

Keywords: electro-discharge process; ethanol; polyvinylpyrrolidone (PVP); silver (Ag); silver nanoparticles (AgNPs)

1. Introduction

In recent years, the synthesis of nanoparticles has been playing a significant role in the production of nano scales due to the improvement of their physical, chemical, biological, optical, and photonic properties (Asgari *et al*. (2022) Arora and Sharma (2014), Babaei *et al*. (2019 a, b), Johnston *et al*. (2010), Asemi *et al*. (2022), Ponnusami *et al*.(2023), Damghanian *et al*. (2020), Rycenga *et al*. (2011), Powers *et al*. (2011), Daryayehsalameh *et al*. (2022), Babaei *et al*. (2021), Kobayashi *et al*. (2017), Low *et al*. (2018), Taj *et al*. (2021), Kiarasi *et al*. (2021a, b, c), Babaei *et al*. (2022a, b, c, d), Mollaei *et al*. (2023), Khatoonabadi *et al*. (2023), Bayat *et al*. (2024), Zhou *et al*. (2023), Babaei *et al*. (2020), Shen *et al*. (2024)). The nanoparticle reinforced composites due to their high strength concurrent with their low weight can be applied for high-tech applications. The demand for nanoparticles in composite structures is largely weighed by the development of the automotive and transportation, aerospace and defense, marine, wind energy and sporting goods end-use industries (Boutaleb *et al*. (2024), Gawah *et al*. (2024), Babaei *et al*. (2024), Alsubaie *et al*. (2024), Huang *et al*. (2021), Tien *et al*. (2023), Kiarasi *et al*. (2022 a, b, c), Cuong *et al*. (2024), Liu *et al*. (2022), Taghizadeh *et al*. (2024), Alsubaie *et al*. (2023), Janghorban and Tounsi (2024), Xia *et al*. (2023), Madenci *et al*. (2023), Zerrouki *et al*. (2024), Zhang *et al*. (2023), Mangalasseri *et al*. (2023), Bi *et al*. (2023), Van Vinh and Tounsi (2022 a, b), Cuong-Le *et al*. (2022), Bouafia *et al*. (2021), Heidari *et al*. (2021), Nazari *et al*. (2021), Wang *et al*. (2023), Liu *et al*. (2024), Shahsavari *et al*. (2021)). Today, silver nano-particles are used in the electronics, optics, chemicals, textiles, pharmaceuticals, cosmetics, as well as food and packaging industries. Silver nanoparticles are used in these industries for producing catalyst materials, sensors, conductors, and detergents (Habouti *et al*. (2010), Hu *et al*. (2004), Alshehri *et al*. (2012), Chen *et al*. (2014), Goodman *et al*. (2014), Braun *et al*. (2014)). Due to the non-toxicity and safety of silver nanoparticles for human and animal cells, these particles are also widely used as an antibacterial agent in the disinfection of hospital equipment. Silver nanoparticles can be produced by physical processes involving electro-discharge and laser processes (Abou El-Nour *et al*. (2010), Tien *et al*. (2008), Kosmala *et al*. (2011), Asanithi *et al*. (2012)), chemical processes such as reduction methods, micro-emulsions, electro-chemicals, and reduction photo-induced (Zhang *et al*. (2011), Roldán *et al*. (2013), Sotiriou and Pratsinis (2010), Sotiriou *et al*. (2011)) or biological processes such as use of eukaryotic fungi as a reducing agent (Shivaji *et al*. (2011), Li *et al*. (2011), Mourato *et al*. (2011), Ge *et al*. (2014)). In this regard, the process of electro-discharge developed between immersed electrodes in liquids has been used as a low cost and simple

*Corresponding author, Professor,
E-mail: farhadkiarsi@eyc.ac.ir
**Co-corresponding author, Professor,
E-mail: Xinyubaii01@163.com

ISSN: 2287-237X (Print), 2287-2388 (Online)

method for the synthesis of nanoparticles of various materials in recent years (Tien *et al*. (2008), Nicolae-Maranciuc *et al*. (2022)). In 2014, Fang and colleagues synthesized titanium oxide nanoparticles with different polymorphic phases using the electro-discharge process (Fang *et al*. (2014)). In another work, Kabirinia *et al*. (2019), investigated the effects of process parameters including the type of gas, gas flow rate, discharge current, and pulse on-time duration on powder production rate and size. Rahaghi *et al* (2015), examined the optical behaviour of synthesized Cu-Ag nanoparticles using the process of electro-discharge between two electrodes of silver and copper. They examined the effect of input parameters of the electro-discharge process on nano-structured tungsten carbide powder synthesized by this method. Sun *et al*. (2016) recently synthesized nano-carbon materials using methods of plasma and an electro-discharge process in dielectric. Burakov *et al*. (2008) utilized the method to synthesize copper nanoparticles encapsulated within a carbon flake, ethyl alcohol for synthesizing tungsten carbide, and water for synthesizing zinc oxide nanoparticles through the electro-discharge process between electrodes of C, Cu, C, W, and Zn, with Zn used in aqueous solution of CuCl2. Lin (2005) produced tungsten carbide nanoparticles successfully by an electro-discharge process between two tungsten and graphite electrodes immersed in a dielectric base of oil and then heat treated it by nitrogen atmosphere. Hu *et al*. (2017) studied the iron nanoparticles encapsulated in the graphite flake using the process of electro-discharge and its morphological properties. In 2017, Safari and colleagues produced nickel ferrite nanoparticles using an electro-discharge process and studied its magnetic properties (Safari *et al*. (2017)).

In this study, silver nanoparticles were produced using the electro-discharge process created between two silver electrodes in four different dielectric types: 1) Ethanol; 2) Ethanol-PVP solution with a concentration of 30mL for PVP; 3) Ethanol-PVP solution with a concentration of 50mL for PVP; and 4) Ethanol-PVP solution with a concentration 80mL for PVP. Further, the effect of adding PVP materials with different concentrations to the dielectric solution of ethanol and changing the process parameters (current intensity (A) and pulse time duration (μs)) was investigated on the structure, phases, size, and production rate of powder produced in these four types of dielectrics and eventually compared.

2. Experimental procedure

2.1 Experiment design and equipment

In this study, the Spark Roboform machine made by Shermills Corporation was utilized to create an electro-discharge process. Also, silver electrodes were employed as an anode and a cathode, and these were put carefully into a dielectric liquid using a special fixture and a container with 0.01 precision. Other specifications of the tests and materials are given in Table 1. PSA machine (Model SZ-100 manufactured by Hariba) was employed to measure the particle size distribution. XRD test was utilized to determine the phases of the produced particles. For this purpose, samples were evaluated by XRD machine, Philips D6792 model, which uses CuKα light with λ=1.54 Å wavelength. The Transmission Electron Microscopy device manufactured by Philips (model CM120) and Scanning Electron Microscopy (JEOL corporation, model JSM6400) were used to investigate the morphological properties of the produced nanoparticles.

Table 1 EDM adjusted Parameters for the production of silver nanoparticles (AgNPs)

Condition and variable	Description
Generator type	Iso pulse
Electrodes Material	Ag (Φ =5mm, L=20mm)
Polarity	Negative
Dielectric	Ethanol and Ethanol-PVP
Stabilizer	PVP (Polyvinylpyrrolidone) with concentrations of 30, 50, and 80mL in 1000mL of Ethanol
Flashing type	Normally submerged without circulation
Depth (mm)	1.0
Gap(mm)	0.09
Finishing capacitor	0
Power available (A)	8,16,32,48 and 64
Pulse time duration (μs)	25,50,100,400
Voltage (v)	200
Duration of interval between tow pulse (μs)	6.4

Table 2 Dielectric constant

Type of material	Ethanol	Polyvinylpyrrolidone
Dielectric constant	24	7

2.2 Materials

Two silver electrodes with a diameter of 5 (mm), a length of 20 (mm), and a purity of 99.95% were used along with ethanol as a dielectric, polyvinylpyrrolidone (PVP) with 360-degree polymerization, and K30 as a stabilizer to produce silver powder in nano dimensions.

2.3 Preparation of dielectric solution

For this purpose, 30, 50, and 80 mL of PVP material were separately mixed in 1000 mL of ethanol as a solvent using a magnetic stirrer for 1 hour at 400 rpm and at 25 °C to prepare an Ethanol-PVP solution with different PVP concentrations as dielectric.

3. Results and discussion

3.1 Effect of the dielectric type on the powder production rate by changing the current intensity

The diagram of the changes in the powder production rate in relation to the current intensity at pulse times

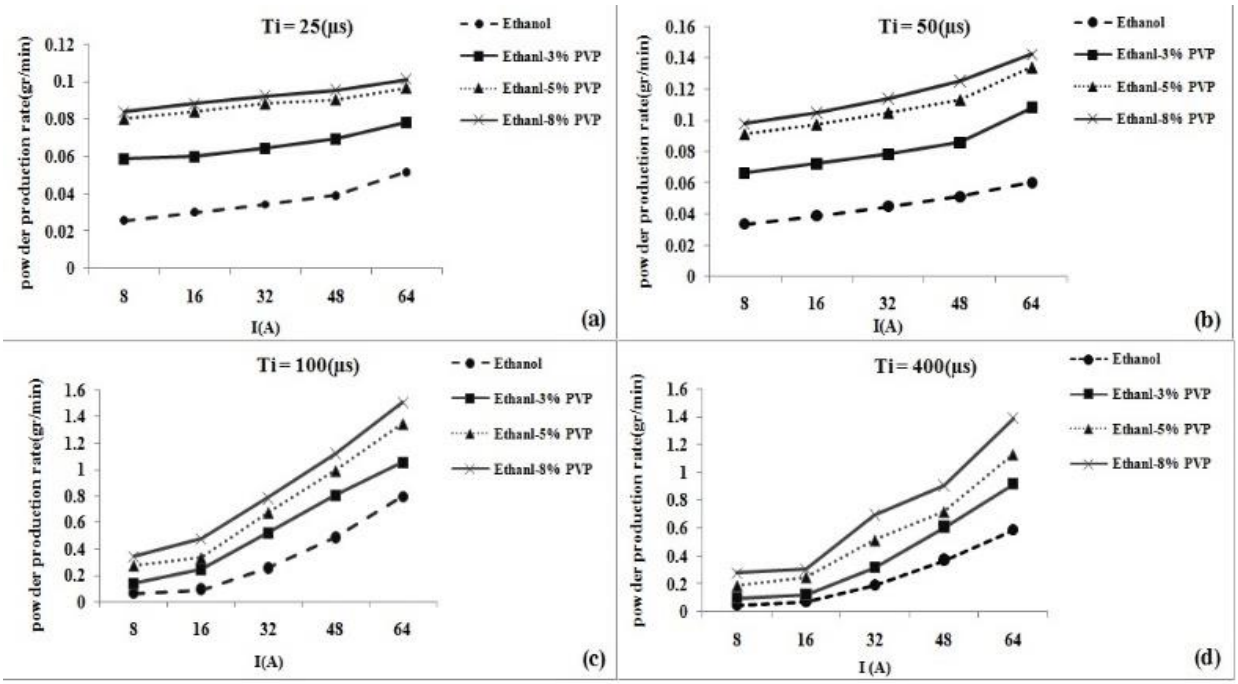

Fig. 1 Changes in the powder rate produced relative to the current intensity at different pulse durations (a) Ti=25 (µs), (b) Ti=50 (µs), (c) Ti=100 (µs) and (d) Ti=400 (µs)

durations of 25, 50, 100, and 400 (µs) for the four dielectric types has been demonstrated in Fig 1. As can be observed, in all four types of pulse time duration by enhancing the current intensity, the production rate of powder grows for all four dielectrics. The reason for this rise can be attributed to the increased energy released in the plasma channel with elevation of the intensity of spark current. According to Formula (1), the average released energy in the plasma channel is affected by factors such as spark voltage (Vsp), spark current intensity (Isp), pulse time duration (Ti), spark delay time (Td), and spark time duration (Tsp) (Jain 2011).

$$W_{ave} = V_{sp} \times I_{sp} (T_i - T_d) = V_{sp} \times I_{sp} \times T_{sp} \quad (1)$$

On the other hand, as can be seen, the powder production rate grows with raising the PVP concentration in ethanol by increasing the current intensity. By augmenting the PVP concentration in the PVP-Ethanol solution, the dielectric constant of the solution (εm) rises. The dielectric constant PVP (Jouyban *et al*. (2004)) and ethanol (Mohsen-Nia *et al*. (2010)) are listed separately in Table 2.

Formula (2) is given to calculate the dielectric constant of a binary solution (Jouyban *et al*. (2004)):

$$\ln \varepsilon_m = \phi_1 \ln \varepsilon_1 + \phi_2 \ln \varepsilon_2 + \phi_1 \phi_2 \sum_{i=0}^{2} k_i (\phi_1 - \phi_2) \quad (2)$$

where, ε_m, ε_1, and ε_2 are the dielectric constants of the mixture and solvents 1 and 2, respectively; ϕ_1 and ϕ_2 are the volume (weight or mole) fractions of solvents 1 and 2 in the mixture; and K_i represents the model constants calculated using a least square method.

According to Formula (2), the dielectric constant (ε_m) grows with increasing the PVP concentration in the ethanol solution. Also, the breakdown voltage of the solution rises with increasing the dielectric constant. According to Formulae (3) and (4), the effect of breakdown voltage on the plasma channel energy and material removal rate is as follows:

$$W = \frac{1}{2} C V_b^2 \quad (3)$$

$$MRR \propto \frac{1}{2} C V_b^2 f_c \quad (4)$$

where, the energy released in the plasma channel is (W), (C) is the capacitor capacity in RC circuit in the electro-discharge process, f_c represents a charge frequency to create plasma, and MRR denotes the material removal rate at which electrodes are ejected during the electro-discharge process.

According to Equations (3) and (4), it is clear that enhancing the PVP concentration in ethanol solution can augment the breakdown voltage of the dielectric solution and the energy released in the plasma channel, thereby elevating the powder production rate in the electro-discharge process.

3.2 The effect of the dielectric type on the powder production rate versus pulse time duration

Fig 2 illustrates the diagram of the changes in the powder production rate versus the pulse time duration at the current intensities of 16, 32, 48 and 64 A for the four dielectric types.

Evidently, the powder production rate in all four current intensities increases with lengthening the pulse time duration up to 100 µs, after which it decreases for T_i=400 µs. Indeed, the reason for increasing the powder production

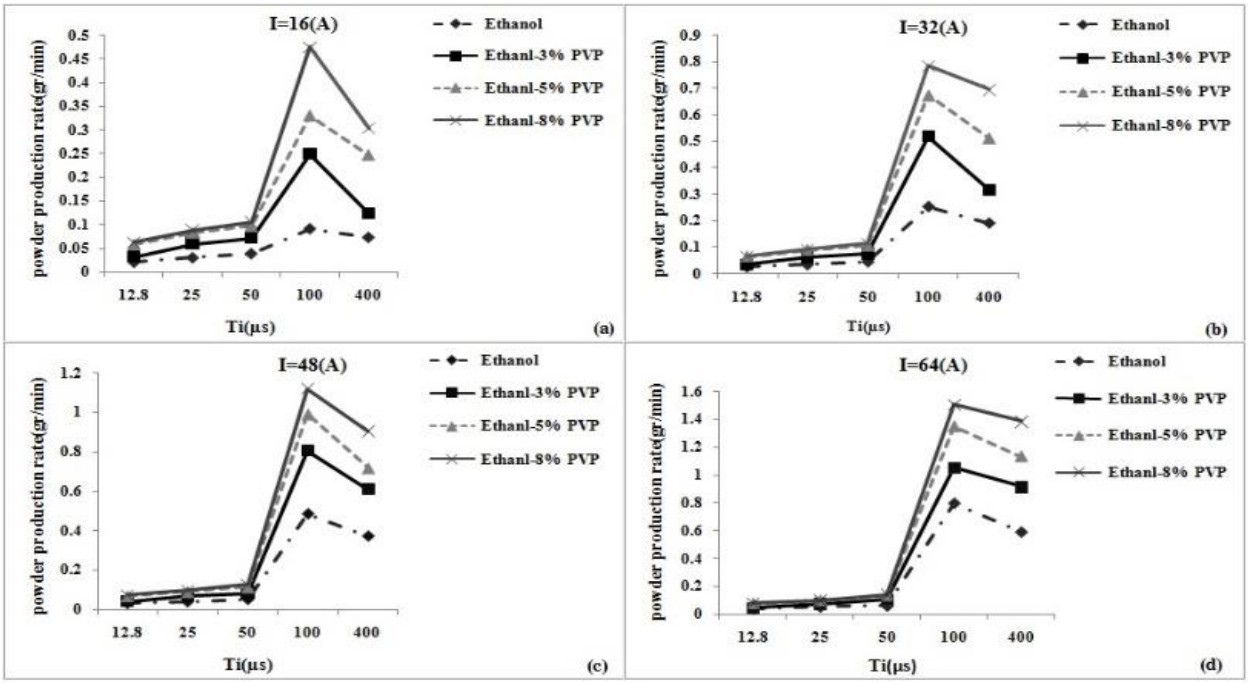

Fig. 2 The changes in the powder production rate versus the pulse duration at the current intensities of: (a) 16 A, (b) 32 A, (c) 48 A, and (d) 64 A

rate up to T_i =100 µs can be attributed to the elevation of spark time duration (T_{sp}), in accordance with Eq. (1). However, according to Eq. (5) (Jain (2011)), the reason for the sudden fall in the powder production rate at T_i=400 µs is related to the reduction of the machining power due to excessive expansion of the plasma channel; the effect of thermodynamic factors such as the drop in the vapor pressure of the detached materials from the surface of the two electrodes; and the reduction of the plasma channel temperature due to the excessive rise in the pulse time duration. Where, T_o is the pulse off time.

$$P_{ave} = \frac{V_{sp} \times I_{sp}(T_i - T_d)}{T_i + T_o} \quad (5)$$

Also, excessive rise of I_{sp} in relation to the pulse time duration can lead to increased density of the metals pollution and the viscosity of the dielectric solution, both of which can cause arc phenomenon during the electro-discharge process, which is also another factor for diminished powder production rate at T_i =400 (µs) (Kabirinia *et al*. (2019).

3.3 Effect of the dielectric type on the particle size distribution at various current intensities and pulse times durations

Fig 3 displays the effect of the dielectric type on the particle size distribution by altering the current intensity and pulse time duration. As can be seen, the size of particles enlarges in dielectric ethanol at a low current intensity of 16 A (Fig 3 (a, b)) by lengthening the pulse time duration. Elevation of the size of particles can be associated with increased cooling time (shutdown) of the plasma channel by enhancing the pulse time duration. It is because in this case the silver steam that is detached off the surfaces of the two electrodes is cooled down in a longer time and at a lower speed. Thus, according to these two reasons, nucleation due to growth of particles and attachment of these particles to each other during the cooling down process diminish and as a result particle with a larger size form.

Nevertheless, in the same dielectric (ethanol) at a high current intensity (64A) according to Fig. 3 (c, d), the size of particles shrinks and the particle size frequency grows with increasing the pulse time duration. In other words, by decreasing the size of particles, the produced powder also becomes more homogeneous. The reason for this reduction can be attributed to the increase in the vapor volume of the metal isolated from the surface of the two electrodes in the plasma channel by augmenting the current intensity and pulse time duration. This is because by heightening the metallic pollution volume which results in increased dielectric pollution, the germination and nucleation centers for producing more particles with smaller size during the cooling process increase. On the other hand, by increasing the metallic pollution in dielectric, the possibility of occurrence of sparks on particles produced in previous sparks can increase. In simple words, sparks occur on metal particles. So, in accordance with Formula (6), we have (Jain (2011)):

$$E = \frac{V_c}{d} \quad (6)$$

On the other hand, the particle size shrinks and the frequency of particles size grows by adding PVP to the dielectric solution. In other words, particles will be more homogeneous and smaller in size. In this process, PVP is used as a stabilizer or protective agent, which has the following structure Fig. 4 (Zhang *et al*. (1996)).

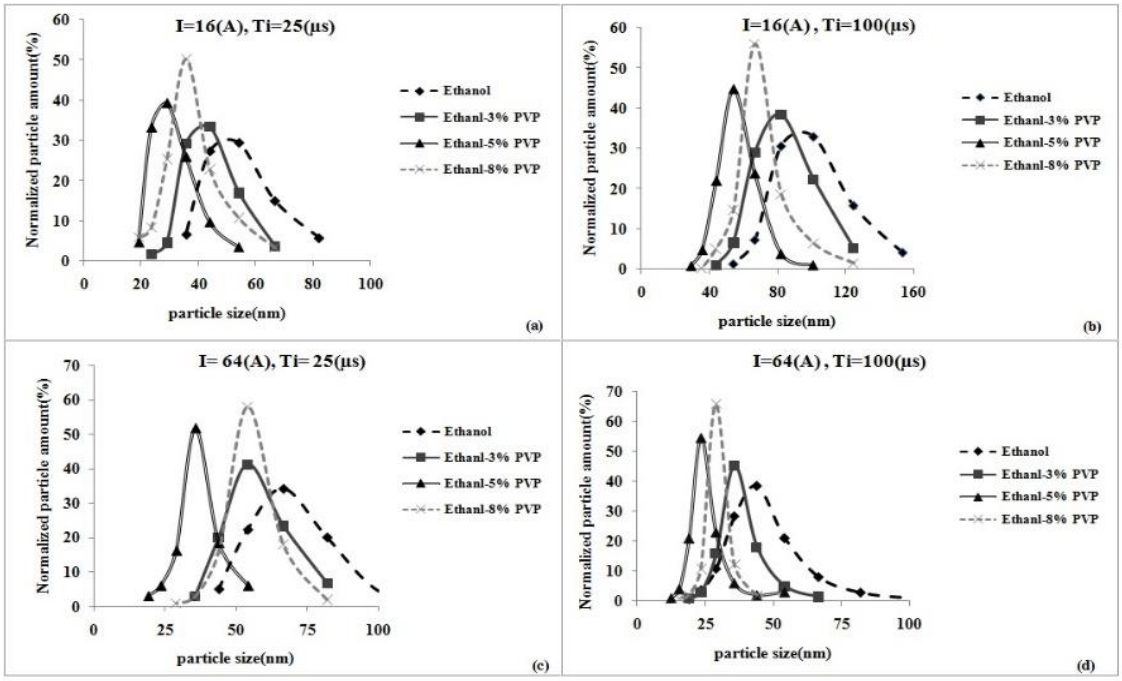

Fig. 3 The effect of dielectric type on the distribution of particle size by changing the pulse intensity and pulse versus time

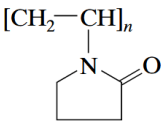

Fig. 4 PVP structure

where, n denotes the number of polymerizations. By adding PVP, the silver ions which are created by the electrical discharge process establish a bond with N or O in PVP. This creates a protective layer on the surface of silver nanoparticles which prevents the formation of a silver-silver band by reducing the number of silver ions. Also, according to Formulae (7) and (8), the ions of silver are stable (Wang *et al*. (2005)):

$$Ag^{+}+PVP \Leftrightarrow Ag(PVP)^{+} \quad (7)$$

$$Ag(PVP) + \ + e - \ \Leftrightarrow Ag(PVP) \quad (8)$$

On the other hand, the agglomeration of silver nanoparticles decreases because of collisions and coalescences between silver ions due to the formation of a protective layer resulting from the bond between O and N formed in the structure of PVP and silver ions on the surface of the particles. Briefly, adding PVP to the dielectric solution increases germination and nucleation of silver nanoparticles (AgNPs) on the one hand and effectively improves and enhances the stability and dispersion of silver nanoparticles on the other. Further, the number of silver ions decreases, and as a result, the silver-silver bond declines with increasing the PVP concentration in the dielectric solution, thereby shrinking the particle size by increasing the concentration of PVP.

Therefore, increasing the concentration of PVP in the

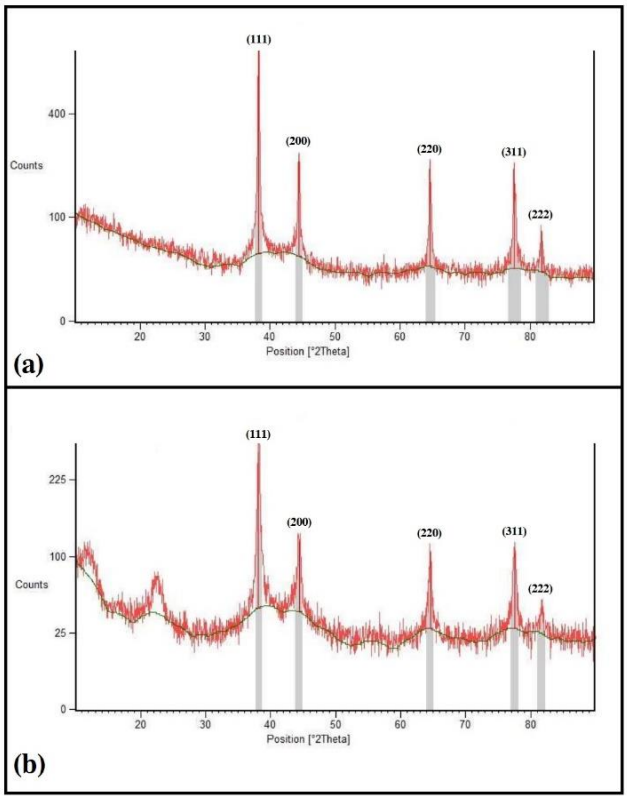

Fig. 5 XRD pattern of the powder produced in (a) dielectric ethanol and (b) dielectric Ethanol-5%mL PVP (current I=64 A and Ti = 100 µs)

Therefore, increasing the concentration of PVP in the dielectric to 50 mL can reduce the size of silver particles across all conditions. However, excessive increase in the PVP material, as can be observed, increases the size of

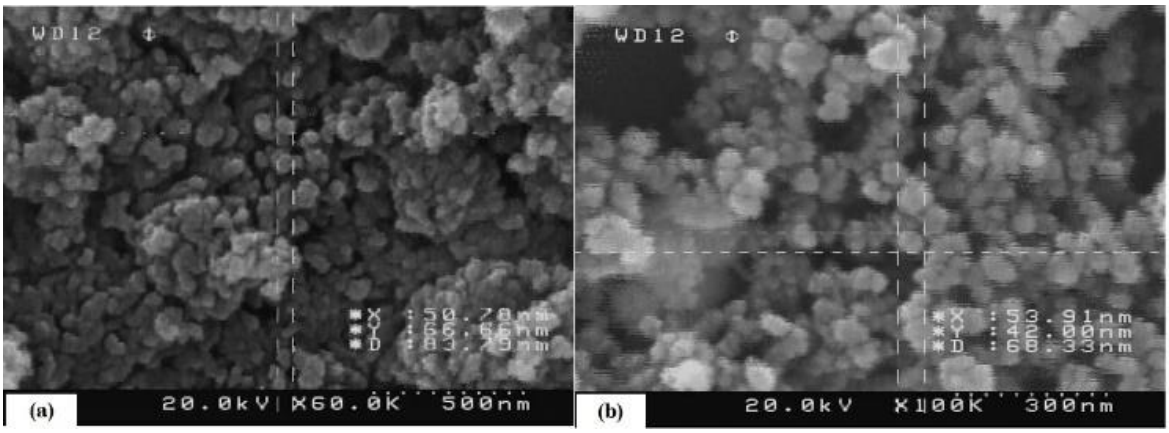

Fig. 6 SEM pictures of the synthesized powders at I= 64 A and Ti= 100 μs : a) Dielectric ethanol and b) Dielectric Ethanol-5% PVP

nanoparticles. The reason for this can be attributed to the excessive reduction in the thermal conductivity of the solution due to the increase of PVP concentration up to 80mL and the decline in the rate of metal vapor cooling in the plasma channel. Therefore, the smallest, most homogeneous silver nanoparticles with the size of 20-45 nm, according to Fig. 3 and with the highest powder production rate according to Figs. 2 and 3 will be created under conditions I=64 A, T_i = 100 μs, and dielectric Ethanol-5% PVP.

3.4 Evaluation of the effect of dielectric type on the structure and powder phase using XRD pattern:

The XRD pattern obtained for dielectric ethanol and Ethanol-5% PVP at I=64 A and T_i = 100 μs is shown in Fig. 5.

According to the XRD patterns for both types of dielectrics, it is clear that the nanoparticles produced by the process of electro-discharge in both cases have an FCC crystal structure (face centered cubic structure). Another point is the absence of oxide phases, especially silver oxide, in both dielectrics. According to Wang *et al*. (2005) and colleagues, nitrogen forms a synthetic reagent with silver ions and a protective layer for particles with a diameter of less than 50 nm, where both N and O elements are bonded with silver ions for particles with diameters larger than 100 nm. As displayed in Fig 3, the particles synthesized by the process of electro-discharge in both dielectrics are smaller than 50 nm. Therefore, we have a reaction according to Formulae (9) and (10) (Wang *et al*. (2005)).

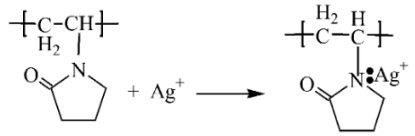

(9)

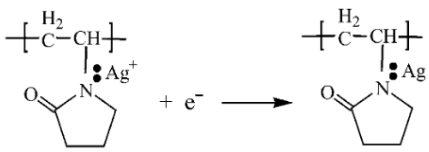

(10)

Accordingly, development of a protective layer on the surface of the nanoparticles due to the high reaction between PVP and silver ions prevents the formation or reduction of unwanted phases. On the other hand, ethanol is decomposed as a result of high temperature as Formula (11) (Zhang and Yu (2013)).

$$CH_3CH_2OH \rightarrow C_2H_4 = +H_2o \quad (11)$$

According to Formula (11), ethanol is decomposed into water and ethene gas (ethylene or ethene). Therefore, there is no possibility of any oxidative phase in this process. Another important point with respect to XRD patterns is that by increasing the concentration of PVP in ethanol, the dielectric diffraction peaks become sharper and shorter in comparison with ethanol dielectric. Also, the intensity of the peaks drops which is the clear reason for the reduction in the size of particles by increasing the concentration of PVP in the dielectric solution.

3.5 Examination of SEM and TEM micrographs

Fig. 6 reveals the SEM graphs representing the morphology of the powder produced in two dielectrics of ethanol and Ethanol-5% PVP for I=64 A and T_i= 100 μs. The reduction in particle size along with the reduction of particle agglomeration is obvious by increasing the concentration of PVP in ethanol. In addition, the powder produced in dielectric Ethanol-5% PVP will be more homogeneous in size than in dielectric ethanol.

The micrographs obtained from TEM are demonstrated in Fig. 7 to examine the morphology of the particles produced in each of the four dielectric types. As can be seen, the core shell structure is observed in all the three dielectrics containing different PVP concentrations by adding PVP to the dielectric. The black areas in the TEMs represent the silver nuclei, which are covered by bright gray areas most likely PVP shells.

The nuclei in the dielectric ethanol in Fig. 7 (a) are not unique in structure but are agglomerated particles. This is due to the silver polarization of the plasma channel. In this case, the silver particles are polarized when they are in the field, where the non-homonymous poles attract each other, causing agglomeration phenomenon and chaining of these

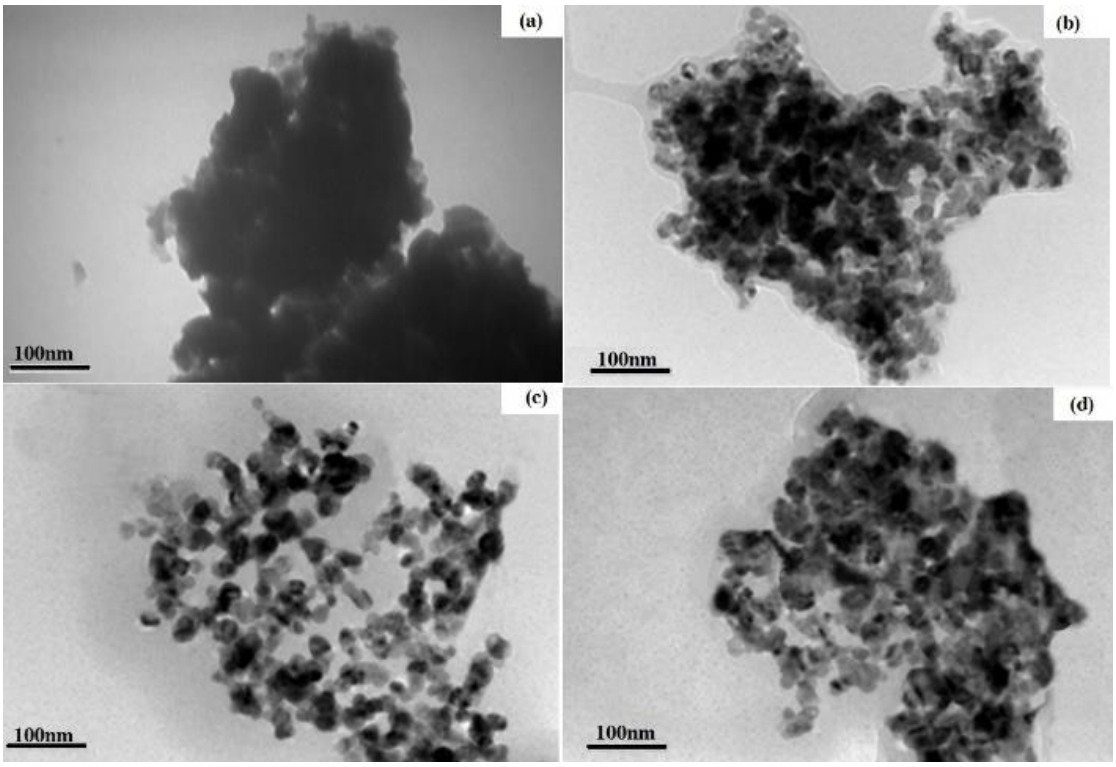

Fig. 7: TEM pictures synthesized powders at I = 64 A and Ti = 100 µs: (a) dielectric ethanol, (b) dielectric ethanol-3% PVP, (c) dielectric ethanol-5% PVP, and (d) dielectric ethanol-8% PVP

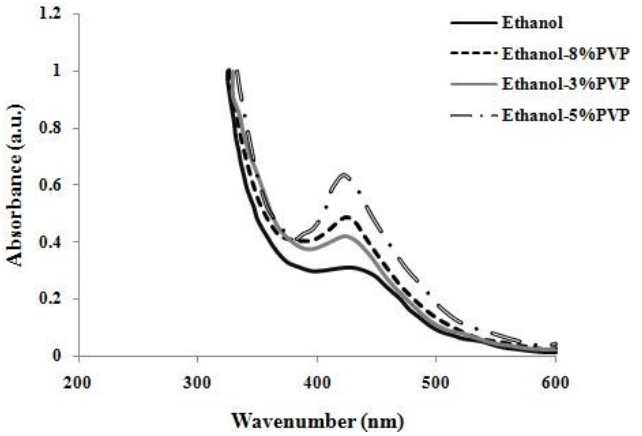

Fig. 8 UV-Vis absorption spectra of the silver nanoparticle samples at I=64 A and Ti=100 µs

particles. Nevertheless, as can be observed, germination and nucleation of silver nanoparticles grows by increasing the concentration of PVP. Also, PVP prevents collision and coalescence like a protective layer, thereby preventing silver-silver bonds and agglomeration, according to Fig. 7 (b, c, and d).

3.6 Examination of UV-Vis absorption spectra of the silver nanoparticle samples

Fig. 8 displays variations of UV-Visible absorption spectra for silver nanoparticles synthesized at I=64 A and T_i=100 µs in dielectrics of ethanol, ethanol-3% PVP, ethanol-5% PVP, and etahnol-8% PVP. As can be seen, the intensity of the surface Plasmon resonance absorption of Ag nanoparticle, at the wavelength of 422 nm, grows with elevation of PVP concentration in ethanol up to 50 ml, but after that it begins to decline. Nevertheless, the maximum absorption site slightly shifts to a shorter wavelength with PVP concentration rise, suggesting production of smaller-sized nanoparticles.

4. Conclusions

In this study, the results of the experiments and investigations on the production of silver nanoparticles using the electro-discharge process in four dielectrics: 1) Ethanol, 2) Ethanol-3% PVP, 3) Ethanol-5% PVP, and 4) Ethanol-8% PVP can be summarized as below:

1. enhanced powder production rate by raising the PVP concentration in ethanol due to increased dielectric breakdown voltage;
2. Increased powder production rate by increasing the current intensity and pulse time duration due to increased energy released in the plasma channel;
3. Reduced size of particles (25nm-50nm) by increasing the PVP concentration to 50mL due to development of a bond between PVP reactive elements and silver ions, thus creating a protective layer on the surface of the silver nanoparticles which reduces collision and coalescence and causes the agglomeration of silver nanoparticles;
4. Enhanced nucleation and particle growth by increasing the PVP concentration in the dielectric;
5. Increased and improved stabilization and dispersion

of silver nanoparticles by raising the concentration of PVP.

6. Prevention from development of undesirable phases such as oxide phases in the synthesis of silver nanoparticles by the electro-discharge process;

7. The optimum conditions for the synthesis of silver nanoparticles with a diameter of 25 nm-50 nm) were I=64 A, T_i = 100 µs, and dielectric with a PVP concentration of 50mL in ethanol.

Acknowledgement

The authors extend their appreciation to the Deanship of Scientific Research at Northern Border University, Arar, KSA for funding this research work through the project number "NBU-FFR-2024-2933-xxx".

References

Abou El-Nour, K.M. Eftaiha, A.A. Al-Warthan, A. and Ammar. R.A. (2010), "Synthesis and applications of silver nano-particles", *Arab. J. Chem.*, **3**(3), 135-140. https://doi.org/10.1016/j.arabjc.2010.04.008

Alshehri, A.H., Jakubowska M., Młożniak, A., Horaczek, M., Rudka, D., Free, C. and Carey, J.D. (2012), "Enhanced electrical conductivity of silver nanoparticles for high frequency electronic applications", *ACS Appl. Mater. Interf.*, **4**(12), 7007-7010. https://doi.org/10.1021/am3022569

Alsubaie, A.M., Alfaqih, I., Al-Osta, M.A., Tounsi, A., Chikh, A., Mudhaffar, I.M. and Tahir, S. (2023), "Porosity-dependent vibration investigation of functionally graded carbon nanotube-reinforced composite beam", *Comput. Concr.*, **32**(1), 75-85. https://doi.org/10.12989/cac.2023.32.1.075

Alsubaie, A.M., Al-Osta, M.A., Alfaqih, I., Tounsi, A., Chikh, A., Mudhaffar, I.M., Al-Dulaijan, S.U. and Tahir, S. (2024), "Influences of porosity distributions on bending and buckling behaviour of functionally graded carbon nanotube-reinforced composite beam", *Comput. Concr.*, **34**(2), 179-193. https://doi.org/10.12989/cac.2024.34.2.179

Arora, N. and Sharma, N. (2014), "Arc discharge synthesis of carbon nanotubes: Comprehensive review", *Diamond Relat. Mater.*, **50**, 135-150. https://doi.org/10.1016/j.diamond.2014.10.001

Asanithi, P., Chaiyakun, S. and Limsuwan, P. (2012), "Growth of silver nanoparticles by DC magnetron sputtering", *J. Nanomater.*, **79**. https://doi.org/10.1155/2012/963609

Asemi, K., Babaei, M. and Kiarasi, F. (2022), "Static, natural frequency and dynamic analyses of functionally graded porous annular sector plates reinforced by graphene platelets", *Mech. Based Des. Struct. Mach.*, **50**(11), 3853-3881. https://doi.org/10.1080/15397734.2020.1822865

Asgari, G.R., Arabali, A., Babaei, M. and Asemi, K. (2022), "Dynamic instability of sandwich beams made of isotropic core and functionally graded graphene platelets-reinforced composite face sheets", *Int. J. Struct. Stabil. Dyn.*, **22**(8), 2250092. https://doi.org/10.1142/S0219455422500924

Babaei, M., Asemi, K. and Safarpour, P. (2019a), "Buckling and static analyses of functionally graded saturated porous thick beam resting on elastic foundation based on higher order beam theory", *Iran. J. Mech. Eng. Transact. ISME*, **20**(1), 94-112.

Babaei, M., Asemi, K. and Safarpour, P. (2019b), "Natural frequency and dynamic analyses of functionally graded saturated porous beam resting on viscoelastic foundation based on higher order beam theory", *J. Solid Mech.*, **11**(3). https://doi.org/10.22034/JSM.2019.666691

Babaei, M. and Asemi, K. (2020), "Static, dynamic and natural frequency analyses of functionally graded carbon nanotube annular sector plates resting on viscoelastic foundation", *SN Appl. Sci.*, **2**(10), 1652. https://doi.org/10.1007/s42452-020-03421-7

Babaei, M., Kiarasi, F., Hossaeini Marashi, S.M., Ebadati, M., Masoumi, F. and Asemi, K. (2021), "Stress wave propagation and natural frequency analysis of functionally graded graphene platelet-reinforced porous joined conical–cylindrical–conical shell", *Waves Random Complex Med.*, 1-33. https://doi.org/10.1080/17455030.2021.2003478

Babaei, M., Kiarasi, F., Tehrani, M.S., Hamzei, A., Mohtarami, E. and Asemi, K. (2022a), "Three dimensional free vibration analysis of functionally graded graphene reinforced composite laminated cylindrical panel", *Proceedings of the Institution of Mechanical Engineers, Part L: Journal of Materials: Design and Applications*, **236**(8), 1501-1514. https://doi.org/10.1177/14644207211073445

Babaei, M. and Asemi, K. (2022b), "Stress analysis of functionally graded saturated porous rotating thick truncated cone", *Mech. Based Des. Struct.*, **50**(5), 1537-1564. https://doi.org/10.1080/15397734.2020.1753536

Babaei, M., Kiarasi, F., Asemi, K. and Hosseini, M. (2022c), "Functionally graded saturated porous structures: A review", *J. Comput. Appl. Mech.*, **53**(2), 297-308. https://doi.org/10.22059/jcamech.2022.342710.719

Babaei, M., Kiarasi, F., Asemi, K., Dimitri, R. and Tornabene, F. (2022d), "Transient thermal stresses in FG porous rotating truncated cones reinforced by graphene platelets", *Appl. Sci.*, **12**(8), 3932. https://doi.org/10.3390/app12083932

Babaei, M., Kiarasi, F. and Asemi, K. (2024), "Torsional buckling response of FG porous thick truncated conical shell panels reinforced by GPLs supporting on Winkler elastic foundation. *Mech. Based Des. Struct.*, **52**(6), 3552-3581. https://doi.org/10.1080/15397734.2023.2205488

Bayat, M.J., Kalhori, A., Babaei, M. and Asemi, K. (2024), "Natural frequency characteristics of stiffened FG multilayer graphene-reinforced composite plate with circular cutout resting on elastic foundation", *Int. J. Struct. Stabil. Dyn.*, **24**(18), 2450202. https://doi.org/10.1142/S021945542450202X

Bi, S., Zhang, E., Babaei, M., Tornabene, F. and Dimitri, R. (2023), "The influence of GPL reinforcements on the post-buckling behavior of FG porous rings subjected to an external pressure", *Mathematics*, **11**(11), 2421. https://doi.org/10.3390/math11112421

Bouafia, H., Chikh, A., Bousahla, A.A., Bourada, F., Heireche, H., Tounsi, A., Benrahou, K.H., Tounsi, A., Al-Zahrani, M.M. and Hussain, M. (2021), "Natural frequencies of FGM nanoplates embedded in an elastic medium", *Adv. Nano Res.*, **11**(3), 239-249. http://doi.org/10.12989/anr.2021.11.3.239

Boutaleb, S., Boulal, A., Zidour, M., Al-Osta, M.A., Tounsi, A., and Tounsi, A. (2024), "On the buckling response of functionally graded carbon nanotube-reinforced composite imperfect beams", *Periodica Polytechnica Civil Eng.*, **68**(4), 1052-1063. https://doi.org/10.3311/PPci.23825

Burakov, V. Savastenko, N. Tarasenko, N. and Nevar, E. (2008), "Synthesis of nanoparticles using a pulsed electrical discharge in a liquid", *J. Appl. Spectroscopy*, **75**(1), 114-124. https://doi.org/10.1007/s10812-008-9003-z

Braun, G.B., Friman, T., Pang, H. B., Pallaoro, A., De Mendoza, T.H., Willmore, A.M.A., Kotamraju, V.R., Mann, A.P., She, Z.G., Sugahara, K.N. (2014), "Etchable plasmonic nanoparticle probes to image and quantify cellular internalization", *Nature Mater.*, **13**(9), 904-911. https://doi.org/10.1038/nmat3982

Chen, G., Lu, J., Lam, C. and Yu, Y. (2014), "A novel green synthesis approach for polymer nanocomposites decorated with

silver nanoparticles and their antibacterial activity", *Analyst*, **139**(22), 5793-5799. https://doi.org/10.1039/C4AN01301H

Cuong-Le, T., Nguyen, K.D., Le-Minh, H., Phan-Vu, P., Nguyen-Trong, P. and Tounsi, A. (2022), "Nonlinear bending analysis of porous sigmoid FGM nanoplate via IGA and nonlocal strain gradient theory", *Adv. Nano Res.*, **12**(5), 441-455. https://doi.org/10.12989/anr.2022.12.5.441

Cuong, B.M., Tounsi, A., Thom, D.V., Hai Van, N.T. and Minh, P.V. (2024), "Finite element modelling for the static bending response of rotating FG-GPLRC beams with geometrical imperfections in thermal mediums", *Comput. Concr.*, **33**(1), 91-102. https://doi.org/10.12989/cac.2024.33.1.091

Damghanian, R., Asemi, K. and Babaei, M. (2020), "A new beam element for static, free and forced vibration responses of microbeams resting on viscoelastic foundation based on modified couple stress and third-order beam theories", *Iranian J. Sci. Technol. Transact. Mech. Eng.*, 1-17. https://doi.org/10.1007/s40997-020-00407-z

Daryayehsalameh, B., Ayari, M.A., Tounsi, A., Khandakar, A. and Vaferi, B. (2022), "Differentiation among stability regimes of alumina-water nanofluids using smart classifiers", *Adv. Nano Res.*, **12**(5), 489-499. https://doi.org/10.12989/anr.2022.12.5.489

Fang, F., Kennedy, J., Carder, D., Futter, J. and Rubanov, S. (2014), "Investigations of near infrared reflective behaviour of TiO2 nanopowders synthesized by arc discharge", *Opt. Mater.*, **36**(7), 1260-1265. https://doi.org/10.1016/j.optmat.2014.03.010

Gawah, Q., Bourada, F., Al-Osta, M.A., Tahir, S.I., Tounsi, A. and Yaylaci, M. (2024), "An improved first-order shear deformation theory for wave propagation analysis in FG-CNTRC beams resting on a viscoelastic substrate", *Int. J. Struct. Stabil. Dyn.*, **25**(1), 2550010. https://doi.org/10.1142/S0219455425500105

Ge, L., Li, Q., Wang, M., Ouyang, J., Li, X. and Xing, M.M. (2014), "Nanosilver particles in medical applications: synthesis, performance, and toxicity", *Int. J. Nanomed.*, **9**, 2399-2403. https://doi.org/10.2147%2FIJN.S55015

Goodman, A.M., Cao, Y., Urban, C., Neumann, O. Ayala-Orozco, C., Knight, M.W., Joshi, A., Nordlander, P. and Halas, N.J. (2014), "The surprising in vivo instability of near-IR-absorbing hollow Au–Ag nanoshells", *Acs Nano*, **8**(4), 3222-3231. https://doi.org/10.1021/nn405663h

Habouti, S., Solterbeck, C.H. and Es-Souni, M. (2010), "Synthesis of silver nano-fir-twigs and application to single molecules detection", *J. Mater. Chem.*, **20**(25), 5215-5219. https://doi.org/10.1039/C0JM00564A

Heidari, F., Taheri, K., Sheybani, M., Janghorban, M. and Tounsi, A. (2021), "On the mechanics of nanocomposites reinforced by wavy/defected/aggregated nanotubes", *Steel Compos. Struct.*, **38**(5), 533-545. http://doi.org/10.12989/scs.2021.38.5.533

Hu, X. and Chan, C. (2004), "Photonic crystals with silver nanowires as a near-infrared superlens", *Appl. Phys. Lett.*, **85**(9), 1520-1522. http://doi.org/10.1063/1.1784883

Hu, R., Furukawa, T., Wang, X. and Nagatsu, M. (2017), "Morphological study of graphite-encapsulated iron composite nanoparticles fabricated by a one-step arc discharge method", *Appl. Surf. Sci.*, **416**, 731-741. https://doi.org/10.1016/j.apsusc.2017.04.231

Huang, Y., Karami, B., Shahsavari, D. and Tounsi, A. (2021), "Static stability analysis of carbon nanotube reinforced polymeric composite doubly curved micro-shell panels", *Archiv. Civil. Mech. Eng.*, **21**, 139. https://doi.org/10.1007/s43452-021-00291-7

Jain, V.K. (2011), *Advanced Machining Processes*, Inderscience Enterprises.

Janghorban, M. and Tounsi, A. (2024), "Two models for wave propagation in polymer/halloysite nanotube nanocomposites: network phenomena/generalized continuum mechanics", *Waves Random Complex Med.*, 1-32. https://doi.org/10.1080/17455030.2024.2396335

Johnston, H.J., Hutchison, G., Christensen, F.M., Peters, S., Hankin, S. and Stone, V. (2010), "A review of the in vivo and in vitro toxicity of silver and gold particulates: particle attributes and biological mechanisms responsible for the observed toxicity", *Critic. Rev. Toxicol.*, **40**(4), 328-346. https://doi.org/10.3109/10408440903453074

Jouyban, A., Soltanpour, S. and Chan, H.K. (2004), "A simple relationship between dielectric constant of mixed solvents with solvent composition and temperature", *Int. J. Pharm.*, **269**(2), 353-360. https://doi.org/10.1016/j.ijpharm.2003.09.010

Kabirinia, F., Shabgard, M. and Salman Tabrizi, N. (2019), "Study on effect of dielectric gas type on electrical discharge erosion synthesis of tungsten carbide nanopowder", *Appl. Phys. A*, **125**(9), 1-10. https://doi.org/10.1007/s00339-019-2888-y

Kiarasi, F., Babaei, M., Sarvi, P., Asemi, K., Hosseini, M. and Omidi Bidgoli, M. (2021a), "A review on functionally graded porous structures reinforced by graphene platelets", *J. Comput. Appl. Mech.*, **52**(4), 731-750. https://doi.org/10.22059/jcamech.2021.335739.675

Kiarasi, F., Babaei, M., Mollaei, S., Mohammadi, M. and Asemi, K. (2021b), "Free vibration analysis of FG porous joined truncated conical-cylindrical shell reinforced by graphene platelets", *Adv. Nano Res.*, **11**(4), 361-380. https://doi.org/10.12989/anr.2021.11.4.361

Kiarasi, F., Babaei, M., Asemi, K., Dimitri, R. and Tornabene, F. (2021c), "Three-dimensional buckling analysis of functionally graded saturated porous rectangular plates under combined loading conditions", *Appl. Sci.*, **11**(21), 10434. https://doi.org/10.3390/app112110434

Kiarasi, F., Asadi, A., Babaei, M., Asemi, K. and Hosseini, M. (2022a), "Dynamic analysis of functionally graded carbon nanotube (FGCNT) reinforced composite beam resting on viscoelastic foundation subjected to impulsive loading", *J. Comput. Appl. Mech.*, **53**(1), 1-23. https://doi.org/10.22059/jcamech.2022.339008.693

Kiarasi, F., Babaei, M., Omidi Bidgoli, M., Reza Kashyzadeh, K. and Asemi, K. (2022b), "Mechanical characterization and creep strengthening of AZ91 magnesium alloy by addition of yttrium oxide nanoparticles", *Proceedings of the Institution of Mechanical Engineers, Part L: Journal of Materials: Design and Applications*, **236**(8), 1489-1500. https://doi.org/10.1177/14644207211073499

Kiarasi, F., Babaei, M., Asemi, K., Dimitri, R. and Tornabene, F. (2022c), "Free vibration analysis of thick annular functionally graded plate integrated with piezo-magneto-electro-elastic layers in a hygrothermal environment", *Appl. Sci.*, **12**(20), 10682. https://doi.org/10.3390/app122010682

Khatoonabadi, M., Jafari, M., Kiarasi, F., Hosseini, M., Babaei, M. and Asemi, K. (2023), "Shear buckling response of FG porous annular sector plate reinforced by graphene platelet subjected to different shear loads", *J. Comput. Appl. Mech.*, **54**(1), 68-86. https://doi.org/10.22059/jcamech.2023.352182.784

Kobayashi, Y., Nakazawa, H., Maeda, T., Yasuda, Y. and Morita, T. (2017), "Synthesis of metallic copper nanoparticles and metal-metal bonding process using them", *Adv. Nano Res.*, **5**(4), 359. https://doi.org/10.12989/anr.2017.5.4.359

Kosmala, A., Wright, R., Zhang, Q. and Kirby, P. (2011), "Synthesis of silver nano particles and fabrication of aqueous Ag inks for inkjet printing", *Mater. Chem. Phys.*, **129**(3), 1075-1080. https://doi.org/10.1016/j.matchemphys.2011.05.064

Kumar, Y., Gupta, A. and Tounsi, A. (2021), "Size-dependent vibration response of porous graded nanostructure with FEM and nonlocal continuum model", *Adv. Nano Res.*, **11**(1), 1-17. http://doi.org/10.12989/anr.2021.11.1.001

Li, G., He, D., Qian, Y., Guan, B., Gao, S., Cui, Y., Yokoyama, K. and Wang. L. (2011), "Fungus-mediated green synthesis of

silver nanoparticles using Aspergillus terreus", *Int. J. Mol. Sci*., **13**(1), 466-476. https://doi.org/10.3390/ijms13010466

Lin, M.H. (2005), "Synthesis of nanophase tungsten carbide by electrical discharge machining", *Ceram. Int*., **31**(8), 1109-1115. https://doi.org/10.1016/j.ceramint.2004.12.004

Liu, G., Wu, S., Shahsavari, D., Karami, B. and Tounsi, A. (2022), "Dynamics of imperfect inhomogeneous nanoplate with exponentially-varying properties resting on viscoelastic foundation", *Eur. J. Mech. A Solids*, **95**, 104649. https://doi.org/10.1016/j.euromechsol.2022.104649

Liu, Z., Tornabene, F., Dimitri, R. and Babaei, M. (2024), "Numerical study of the buckling response of stiffened FG graphene-reinforced multilayer composite cylindrical panels", *Processes*, **12**(3), 430. https://doi.org/10.3390/pr12030430

Low, S. and Shon, Y.S. (2018), "Molecular interactions between pre-formed metal nanoparticles and graphene families", *Adv. Nano Res*., **6**(4), 357. https://doi.org/10.12989/anr.2018.6.4.357

Zhang, Q., Li, N., Goebl, J., Lu, Z. and Yin, Y. (2011), "A systematic study of the synthesis of silver nanoplates: is citrate a magic reagent", *J. Am. Chem. Soc*., **133**(46), 18931-18939. https://doi.org/10.1021/ja2080345

Mangalasseri, A.S., Mahesh, V., Mukunda, S., Mahesh, V., Ponnusami, S.A., Harursampath, D. and Tounsi, A. (2023), "Vibration based energy harvesting performance of magneto-electro-elastic beams reinforced with carbon nanotubes", *Adv. Nano Res*., **14**(1), 27-43. https://doi.org/10.12989/anr.2023.14.1.027

Madenci, E., Özkiliç, Y.O., Hakamy, A. and Tounsi, A. (2023), "Experimental tensile test and micro-mechanic investigation on carbon nanotube reinforced carbon fiber composite beams", *Adv. Nano Res*., **14**(5), 443-450. https://doi.org/10.12989/anr.2023.14.5.443

Mohsen-Nia, M., Amiri, H. and Jazi, B. (2010), "Dielectric constants of water, methanol, ethanol, butanol and acetone: measurement and computational study", *J. Solution Chem*., **39**(5), 701-708. https://doi.org/10.1007/s10953-010-9538-5

Mollaei, S., Babaei, M. and Asemi, K. (2023), "Torsional buckling of functionally graded graphene reinforced composite laminated cylindrical panel", *Arch. Appl. Mech*., **93**(2), 427-435. https://doi.org/10.1007/s00419-022-02132-2

Mourato, A., Gadanho, M., Lino, A.R. and Tenreiro, R. (2011), "Biosynthesis of crystalline silver and gold nanoparticles by extremophilic yeasts", *Bioinorgan. Chem. Appl*., **8**, 1565-3633. https://doi.org/10.1155/2011/546074

Nazari, H., Babaei, M., Kiarasi, F. and Asemi, K. (2021), "Geometrically nonlinear dynamic analysis of functionally graded material plate excited by a moving load applying first-order shear deformation theory via generalized differential quadrature method", *SN Appl. Sci*., **3**, 1-32. https://doi.org/10.1007/s42452-021-04825-9

Nicolae-Maranciuc, A., Chicea, D. and Chicea, L.M. (2022), "Ag nanoparticles for biomedical applications—Synthesis and Characterization—A Review", *Int. J. Mol. Sci*., **23**(10), 5778-5785. https://doi.org/10.3390/ijms23105778

Ponnusami, S.A., Harursampath, D. and Tounsi, A. (2023), "Vibration based energy harvesting performance of magneto-electro-elastic beams reinforced with carbon nanotubes". *Adv. Nano Res*., **14**(1), 27-43. https://doi.org/10.12989/anr.2023.14.1.027

Powers, C.M., Badireddy, A.R., Ryde, I.T., Seidler, F.J. and Slotkin, T.A. (2011), "Silver nanoparticles compromise neuro-development in PC12 cells: critical contributions of silver ion, particle size, coating, and composition", *Environ. Health Perspect*., **119**(1), 37-44. https://doi.org/10.1289/ehp.1002337

Rahaghi, S.H., Poursalehi, R. and Miresmaeili. R. (2015), "Optical properties of Ag-Cu alloy nanoparticles synthesized by DC arc discharge in liquid", *Procedia Materials Science*, **11**, 738-742. https://doi.org/10.1016/j.mspro.2015.11.062

Roldán, M., Pellegri, N. and de Sanctis, O. (2013), "Electro-chemical method for Ag-PEG nanoparticles synthesis", *J. Nanopart*., **2013**(1), 524150. http://doi.org/10.1155/2013/524150

Rycenga, M., Cobley, C. M., Zeng, J., Li, W., Moran, C.H., Zhang, Q., Qin, D. and Xia, Y. (2011), "Controlling the synthesis and assembly of silver nanostructures for plasmonic applications", *Chem. Rev*., **111**(6), 3669-3712. https://doi.org/10.1021/cr100275d

Safari, A., Gheisari, K. and Farbod, M. (2017), "Characterization of Ni ferrites powders prepared by plasma arc discharge process, Journal of Magnetism and Magnetic Materials", *J. Magn. Magn. Mater*., **421**, 44-51. https://doi.org/10.1016/j.jmmm.2016.07.024

Shahsavari, M., Asemi, K., Babaei, M. and Kiarasi, F. (2021), "Numerical investigation on thermal post-buckling of annular sector plates made of FGM via 3D finite element method", *Mech. Adv. Compos. Struct*., **8**(2), 309-320. https://doi.org/10.22075/macs.2021.21158.1293

Shen, X., Li, T., Xu, L., Kiarasi, F., Babaei, M. and Asemi, K. (2024), "Free vibration analysis of FG porous spherical cap reinforced by graphene platelet resting on Winkler foundation. *Adv. Nano Res*., **16**(1), 11. https://doi.org/10.12989/anr.2024.16.1.011

Shivaji, S., Madhu, S. and Singh. S. (2011), "Extracellular synthesis of antibacterial silver nanoparticles using psychrophilic bacteria", *Proc. Biochem*., **46**(9), 1800-1807, https://doi.org/10.1016/j.procbio.2011.06.008

Sotiriou, G.A. and Pratsinis, S. E. (2010), "Antibacterial activity of nanosilver ions and particles", *Environ. Sci. Technol*., **44**(14), 5649-5654. https://doi.org/10.1021/es101072s

Sotiriou, G.A., Teleki, A., Camenzind, A., Krumeich, F., Meyer, A., Panke, S. and Pratsinis, S.E. (2011), "Nanosilver on nanostructured silica: Antibacterial activity and Ag surface area", *Chem. Eng. J*., **170**(2-3), 547-554. https://doi.org/10.1016/j.cej.2011.01.099

Sun, D., Hong, R., Wang, F., Liu, J. and Kumar, M.R. (2016), "Synthesis and modification of carbon nanomaterials via AC arc and dielectric barrier discharge plasma", *Chem. Eng. J*., **283**, 9-20. https://doi.org/10.1016/j.cej.2015.07.023

Taghizadeh, M., Babaei, M., Dimitri, R. and Tornabene, F. (2024), "Assessment of critical buckling load of bi-directional functionally graded truncated conical micro-shells using modified couple stress theory and Ritz method", *Mech. Based Des. Struct*., **52**(6), 3456-3487. https://doi.org/10.1080/15397734.2023.2202230

Taj, M., Khadimallah, M.A., Hussain, M., Elbahar, M., Ahmad, M., Elimame, E. and Tounsi, A. (2021), "An investigation of mechanical properties of kidney tissues by using mechanical bidomain model", *Adv. Nano Res*., **11**(2), 193-201. https://doi.org/10.12989/anr.2021.11.2.193

Tien, D.C., Tseng, K.H., Liao, C.Y., Huang, J.C. and Tsung, T.T. (2008), "Discovery of ionic silver in silver nanoparticle suspension fabricated by arc discharge method", *J. Alloys Compd*., **463**(1-2), 408-411. https://doi.org/10.1016/j.jallcom.2007.09.048

Tien, D.M., Thom, D.V., Thi Hai Van, N., Tounsi, A., Minh, P.V. and Mai, D.N. (2023), "Buckling and forced oscillation of organic nanoplates taking the structural drag coefficient into account", *Comput. Concr*., **32**(6), 553-565. https://doi.org/10.12989/cac.2023.32.6.553

Van Vinh, P. and Tounsi, A. (2022a), "The role of spatial variation of the nonlocal parameter on the free vibration of functionally graded sandwich nanoplates", *Eng. Comput*., **38**, 4301-4319. https://doi.org/10.1007/s00366-021-01475-8

Van Vinh, P. and Tounsi, A. (2022b), "Free vibration analysis of functionally graded doubly curved nanoshells using nonlocal first-order shear deformation theory with variable nonlocal parameters", *Thin Wall. Struct.*, **174**, 109084. https://doi.org/10.1016/j.tws.2022.109084

Wang, H., Qiao, X., Chen, J., Wang, X. and Ding, S. (2005), "Mechanisms of PVP in the preparation of silver nanoparticles", *Mater. Chem. Phys.*, **94**(2-3), 449-453. https://doi.org/10.1016/j.matchemphys.2005.05.005

Wang, X., Guo, X., Babaei, M., Fili, R. and Farahani, H. (2023), "Natural frequency analysis of joined conical-cylindrical-conical shells made of graphene platelet reinforced composite resting on Winkler elastic foundation", *Adv. Nano Res.*, **15**(4), 367-384. https://doi.org/10.12989/anr.2023.15.4.367

Xia, L., Wang, R., Chen, G., Asemi, K. and Tounsi, A. (2023), "The finite element method for dynamics of FG porous truncated conical panels reinforced with graphene platelets based on the 3-D elasticity", *Adv. Nano Res.*, **14**(4), 375-389. https://doi.org/10.12989/.2023.14.4.375

Zerrouki, R., Zidour, M., Tounsi, A., Tounsi, A., Belabed, Z., Bousahla, A.A., ... & Khedher, K.M. (2024), "Buckling behavior of nonlinear FG-CNT reinforced nanocomposite beam reposed on Winkler/Pasternak foundation", *Comput. Concr.*, **34**(3), 297-305. https://doi.org/10.12989/cac.2024.34.3.297

Zhang, Z., Zhao, B. and Hu, L. (1996), "PVP protective mechanism of ultrafine silver powder synthesized by chemical reduction processes", *J. Solid State Chem.*, **121**(1), 105-110. https://doi.org/10.1006/jssc.1996.0015

Zhang, M. and Yu, Y. (2013), "Dehydration of ethanol to ethylene", *Ind. Eng. Chem. Res.*, **52**(28), 9505-9514. https://doi.org/10.1021/ie401157c

Zhang, Y.W., Ding, H.X., She, G.L. and Tounsi, A. (2023), "Wave propagation of CNTRC beams resting on elastic foundation based on various higher-order beam theories", *Geomech. Eng.*, **33**(4), 381-391. https://doi.org/10.12989/gae.2023.33.4.381

Zhou, Y., Zhang, Y., Nyasha Chirukam, B., Li, J., Lu, C., Babaei, M. and Asemi, K. (2023), " Free vibration analyses of stiffened functionally graded graphene-reinforced composite multilayer cylindrical panel", *Mathematics*, **11**(17), 3662. https://doi.org/10.3390/math1117366

CC